



Novel histone deacetylase 8 ligands without a zinc chelating group: Exploring an ‘upside-down’ binding pose

Aditya Sudheer Vaidya^{a,†}, Raghupathi Neelarapu^{a,†}, Antonett Madriaga^a, He Bai^a, Emma Mendonca^b, Hazem Abdelkarim^a, Richard B. van Breemen^a, Sylvie Y. Blond^c, Pavel A. Petukhov^{a,*}

^a Department of Medicinal Chemistry and Pharmacognosy, College of Pharmacy, University of Illinois at Chicago, 833 South Wood Street, Chicago, IL 60612, United States

^b Department of Bioengineering, University of Illinois at Chicago, 851 South Morgan Street, Chicago, IL 60607, United States

^c Center for Pharmaceutical Biotechnology, University of Illinois at Chicago, 900 South Ashland Avenue, Chicago, IL 60612, United States

ARTICLE INFO

Article history:

Received 16 July 2012

Revised 23 August 2012

Accepted 28 August 2012

Available online 7 September 2012

Keywords:

HDAC8

Upside down

Photolabeling

Zinc chelating group

Secondary binding site

ABSTRACT

A novel series of HDAC8 inhibitors without a zinc-chelating hydroxamic acid moiety is reported. Photoaffinity labeling and molecular modeling studies suggest that these ligands are likely to bind in an ‘upside-down’ fashion in a secondary binding site proximal to the main catalytic site. The most potent ligand in the series exhibits an IC₅₀ of 28 μM for HDAC8 and is found to inhibit the deacetylation of H4 but not α-tubulin in SH-SY5Y cell line.

© 2012 Elsevier Ltd. All rights reserved.

Histone deacetylases (HDAC) are considered as promising therapeutic targets.^{1,2} The vast majority of the HDAC inhibitors contains a zinc chelating group (ZCG) as an essential part responsible for their binding affinity. The most commonly used ZCG in HDAC inhibitors is a hydroxamic acid group that shows poor metabolic stability in vivo and is rapidly hydrolyzed to carboxylic acid, a poor ZCG, and hydroxylamine.^{3,4} Compounds containing hydroxamic acid moieties are poorly absorbed in vivo and show extensive glucuronidation and sulfation.⁵ The sulfate conjugates of hydroxamic acids may lead to formation of electrophiles such as isocyanates which may further react with nucleophiles in proteins and other biological macromolecules.^{6–8} Non-hydroxamate ZCGs typically include carboxylic acids (sodium valproate), epoxy ketones (trapoxin), *o*-amino anilides (MS 275), electrophilic ketones, and thiols.^{9–12} These non-hydroxamate ZCGs often suffer from poor potency,¹³ redox activity,¹⁴ general reactivity,¹⁰ metabolic instability,¹⁵ and poor aqueous solubility.¹⁵ For life-long applications, for example as a potential treatment of Alzheimer's disease,^{16,17} these types of properties of HDAC inhibitors are highly undesirable. Clearly, there is an urgent need for the development of HDAC inhibitors that may utilize novel binding modes that do not require a ZCG. A series of non-selective tetrapeptides likely not

chelating to the active site Zn²⁺ of HDAC1–3 is the only example of the non-ZCG HDAC ligands we could find.¹⁸

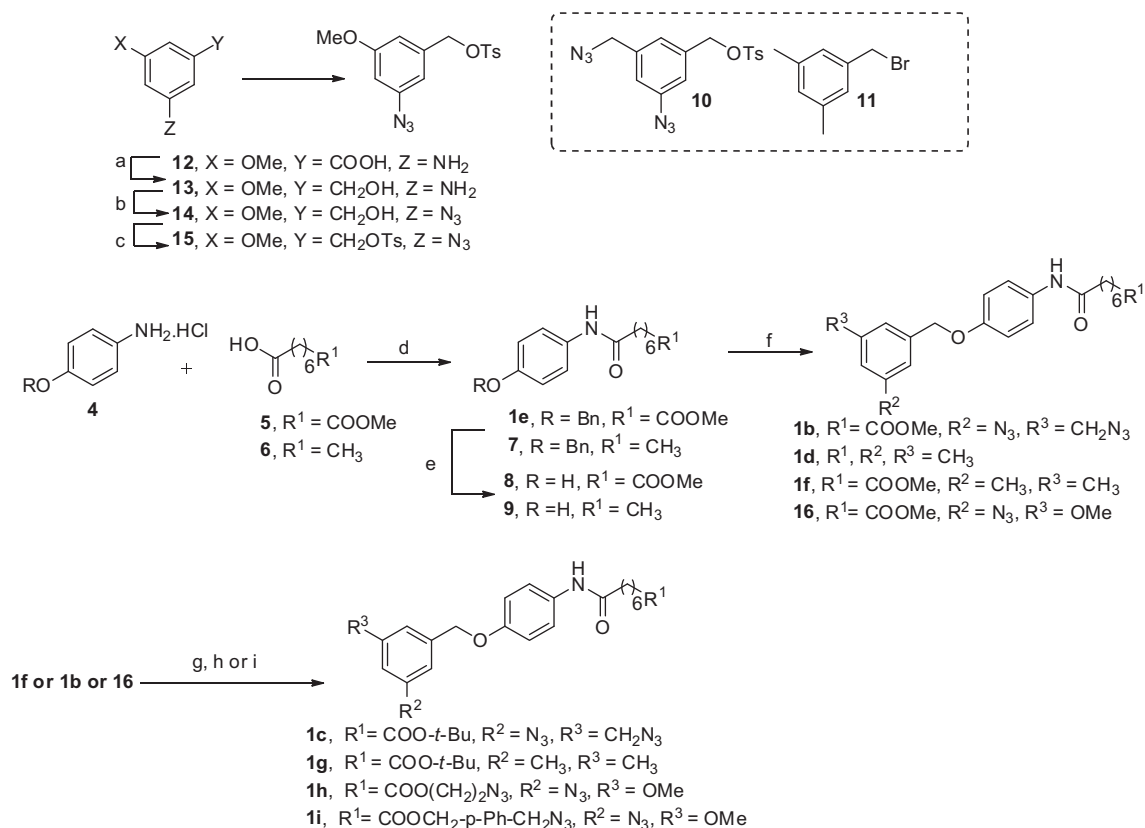
Recently, we have published the Binding Ensemble Profiling with Photoaffinity Labeling (BEProFL) approach that was used to map experimentally the multiple binding poses of the surface binding groups (SBG) of inhibitors of HDAC8,¹⁹ a novel therapeutic target for neuroblastoma,^{20–24} leukemia,²⁵ and cognitive disorders.²⁶ In our paper¹⁹ we noted that some of the covalent modifications of HDAC8 may correspond to a novel ‘upside-down’ pose of the diazide probe that was strikingly similar to that found in HDAC8 (PDB:1T64)²⁷ for one of the two molecules of Trichostatin A bound to the secondary site proximal to the main catalytic site. Our main objective in this study was to design and synthesize a series of diazide-based probes/ligands lacking the hydroxamic acid moiety, test HDAC8 inhibition by these probes, and explore using photoaffinity labeling studies if they bind in an ‘upside-down’ fashion in the secondary binding site in HDAC8.

The synthesis of the ligands/probes is outlined in Scheme 1. Commercially available 4-benzyloxyaniline hydrochloride **4** was coupled with suberic acid monomethyl ester **5** or octanoic acid **6** using a facile carbodiimide based coupling reaction. The benzylhydroxy group of **1e** and **7** was deprotected via catalytic hydrogenation and later coupled with bromide **11** or tosylates **10** and **15**. Esters **1b**, **1f**, and **16** were subjected to basic hydrolysis and re-esterified with appropriate alcohols resulting in probes **1c**, **1g**, **1h**, and **1i**, respectively, in 20–65% overall yields. The structures

* Corresponding author. Tel.: +1 312 996 4174; fax: +1 312 996 7107.

E-mail address: pap4@uic.edu (P.A. Petukhov).

† These authors contributed equally to the work.



Scheme 1. Reagents and conditions (a) LAH, THF, 0 °C to rt; (b) NaNO₂, HCl(aq), NaN₃, 0 °C to rt; (c) TsCl, Et₃N, CH₂Cl₂, 0 °C; (d) suberic acid monomethyl ester or octanoic acid, EDCI, HOBT, DIPEA, CH₂Cl₂, 0 °C to rt; (e) Pd/C, MeOH, rt; (f) **10** or **11** or **15**, K₂CO₃, acetone, reflux; (g) NaOH(aq) or KOH(aq), rt (h) (COCl)₂, *t*-BuOH, DMF, Et₃N, CH₂Cl₂; (i) [4-(azidomethyl)phenyl]methanol or 2-azidoethanol, EDCI, HOBT, CH₂Cl₂, 0 °C to rt.

of the final compounds were elucidated by NMR and confirmed by HRMS.²⁸ Synthetic procedures and data for compounds **1a**, **1b**, **1e**, and **8** and **2a**, **2b**, **3a**, **3b**, and **10** were previously reported by us.^{19,29} [4-(Azidomethyl)phenyl]methanol and 2-azidoethanol were synthesized according to the reported methods.^{30,31}

The inhibition by the probes/ligands was measured using commercially available recombinant human HDAC1, 2, 3, and HDAC8 using fluorogenic substrates Boc-Lys(Ac)-AMC for HDAC1, 2, and 3 and Fluor de Lys for HDAC8, respectively, using previously reported procedures.^{19,29} The resulting IC₅₀ values are given in Table 1. The analysis of the SAR was facilitated by docking of the ligands to HDAC8 (PDB:1T64)²⁷ using GOLD v.5.1.³² and the docking procedure reported by us previously.³³

At first, we replaced the hydroxamic acid moiety in **1a** with a methyl ester and found that ligand **1b** is able to maintain its HDAC8 inhibitory properties (IC₅₀ of **1b** is 37.4 μM) despite the lack of a chemical moiety that can serve as a bidentate chelator to Zn²⁺ (Table 1). Although encouraging, this finding needed further proof that the ester group of ligand **1b** does not serve as a monodentate ZCG. Our preliminary modeling studies have shown that a *t*-butyl ester moiety instead of the methyl ester in **1b** would not be able to fit the binding site of HDAC8 because it is too bulky. The corresponding *t*-butyl ester **1c** was found to inhibit HDAC8 with an IC₅₀ of 42.6 μM, which is similar to that of ligand **1b**. Docking showed that ligand **1c** can only fit the binding site by adopting an 'upside-down' pose shown in Figure 1.

Next, we removed the ester group in **1b**. The resulting ligand **1d** with a rather flexible unsubstituted alkyl chain was found to be inactive. If the binding mode of **1d** is similar to that of **1c**, its long alkyl chain substituent would be solvent exposed and may not contribute to the binding. Thus, lack of potency comparable to that of **1b** appears to be in line in the proposed binding mode.

To explore if the presence of the two lipophilic azide groups is required, we synthesized compound **1e** where hydrogen atoms were placed in both the meta positions in the terminal phenyl ring. Compound **1e** was found to be inactive up to 66 μM. The analysis of the binding site available to the ligands in those HDAC8 X-ray structures where the second copy or an empty binding site adjacent to the catalytic site is present showed that the second pocket is relatively large and there are two additional lipophilic sub-pockets at the bottom. Our docking experiments suggested that in the case of ligands **1a–c** their *meta*-azido and *meta*-methylene azido moieties can occupy these two lipophilic sub-pockets and form extensive hydrophobic interactions with the binding site. In the case of **1e** such interactions were missing. Next, to further verify if the presence of *meta* substituents is required, we synthesized compound **1f** that has two *meta*-methyl substituents in the terminal phenyl ring. The HDAC8 inhibitory potency of **1f** was restored to the level of ligands **1a–d**. The strong dependence on the presence of additional substituents in the terminal phenyl ring is consistent with the 'upside-down' pose where extended interactions with the binding site would be necessary to compensate for the missing interactions between the ZCG and the active site Zn²⁺. In agreement with the proposed 'upside-down' binding pose and the data for esters **1b** and **1c**, potency of the substantially bulkier *t*-butyl ester **1g** is only marginally lower than that of the corresponding methyl ester **1f**. Comparable potency of diazides **1b** and **1c** with dimethyl-substituted **1g** and **1f** indicates that the azide moieties do not form an R-N₃ ··· Zn²⁺ complex if the ligands bind 'upside-down'.

To confirm that the scaffold containing the terminal phenyl ring with two lipophilic meta substituents is, indeed, a universal feature responsible for activity, we synthesized and tested methyl ester derivatives of the diazide probes **2a** and **3a**.⁷ Both **2a** and **3a** are

Table 1
HDAC8 IC₅₀ values for compounds **1a–h**, **2a–b**, and **3a–b**

Compd #	R ¹	R ²	R ³	HDAC8 IC ₅₀ (μM)
1a ^a	CONHOH	N ₃	CH ₂ N ₃	7.34 ± 0.22
1b	COOCH ₃	N ₃	CH ₂ N ₃	37.4 ± 2.34
1c	COO- <i>t</i> -Bu	N ₃	CH ₂ N ₃	42.6 ± 1.81
1d	CH ₃	CH ₃	CH ₃	NA
1e	COOCH ₃	H	H	NA ^d
1f	COOCH ₃	CH ₃	CH ₃	47.8 ± 2.35
1g	COO- <i>t</i> -Bu	CH ₃	CH ₃	53.2 ± 6.49
1h	COOCH ₂ CH ₂ N ₃	N ₃	OCH ₃	67.5 ± 4.79 ^e
1i	COOCH ₂ - <i>p</i> -Ph-CH ₂ N ₃	N ₃	OCH ₃	28.0 ± 2.65 ^f
2a ^b	CONHOH	N ₃	CH ₂ N ₃	0.017 ± 0.003
2b	COOCH ₃	N ₃	CH ₂ N ₃	36.0 ± 2.20
3a ^c	CONHOH	N ₃	CH ₂ N ₃	0.651 ± 0.12
3b	COOCH ₃	N ₃	CH ₂ N ₃	47.1 ± 1.76
SAHA	—	—	—	0.44 ± 0.021 ⁷
TSA	—	—	—	0.39 ± 0.018
PCI34051	—	—	—	0.01 ²⁵

^a HDAC3 IC₅₀ 1.48 μM, K_i 0.74 μM.

^b HDAC3 IC₅₀ 128 nM, K_i 0.064 μM.

^c HDAC3 IC₅₀ 45 nM, K_i 0.023 μM.

^d The residual activity is more than 50% at 66 μM, IC₅₀ was not determined.

^e HDAC1 IC₅₀ 111 ± 14.8 μM, HDAC2 IC₅₀ 72 ± 2.2 μM.

^f HDAC1 IC₅₀ 86.0 ± 7.1 μM, HDAC2 IC₅₀ 79 ± 3.0 μM.

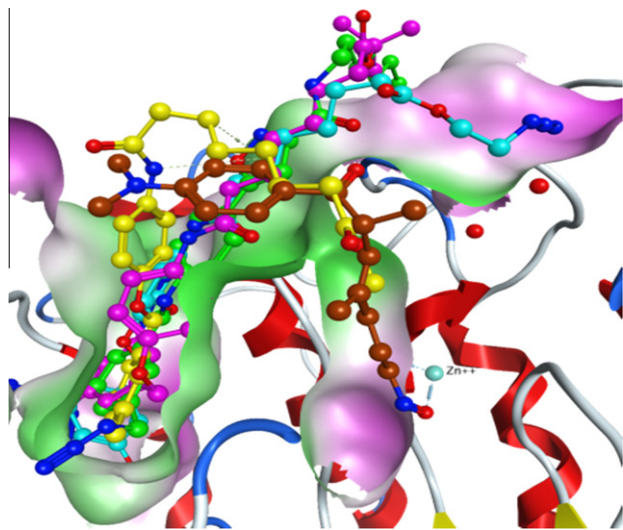


Figure 1. 'Upside-down' binding pose proposed for HDAC8 inhibitors **1c** (magenta), **1f** (yellow), **1h** (cyan), and **3b** (green). TSA bound to the main catalytic site (PDB: 1T64) is rendered brown. The binding site is rendered by solvent accessible surface, green—lipophilic, magenta—hydrophilic.

nanomolar inhibitors of HDAC8. In these ligands the SBG contains a pyrazole or an isoxazole moiety, respectively, as well as the *meta*-azido and *meta*-methyleneazido substituted phenyl ring. Consistently with the 'upside-down' hypothesis, both esters **2b** and **3b**

were found to inhibit HDAC8 with IC₅₀ of 36.0 and 47.1 μM, respectively, which is comparable to the potency of compounds in series **1**. Relatively a small difference in the potency of **2b** and **3b** and similar compounds in series **1** is consistent with the binding pose of the ligands without ZCG (Fig. 1). The terminal phenyl ring of **2b** and **3b** is completely immersed in the binding site whereas the pyrazole and the isoxazole portions of **2b** and **3b**, respectively, are only partially enclosed in the binding site but otherwise are solvent exposed.

Next, we performed a series of photolabeling experiments with purified recombinant HDAC8 to further delineate the putative binding modes of the probes.³⁴ In all the photolabeling experiments, the concentration of purified HDAC8 used was 0.5 μM, and all the experiments were performed in non-denaturing conditions unless otherwise stated. The probe or probe/competitor mixtures were preincubated with purified recombinant HDAC8 from *E. coli*,³⁵ in photolabeling buffer for 3 h at room temperature, exposed to 254 nm UV light for 3 × 1 min with 1 min resting. In case of denaturation experiments, after photoirradiation a solution of sodium dodecyl sulfate was added to attain a final concentration of 2% w/v and the mixture incubated at 37 °C for 30 min. In all photolabeling experiments an alkyne containing biotin tag¹⁹ was attached to the HDAC8-probe adduct using Cu(I) catalyzed (3+2) cycloaddition reaction carried out at room temperature for 1 h. The biotinylated HDAC8 was visualized by streptavidin–HRP and western blot and the loading was confirmed by using anti-HDAC8 antibody. The control wells contained purified HDAC8, a mixture of HDAC8 and the biotin tag, or a mixture of HDAC8 and the probes

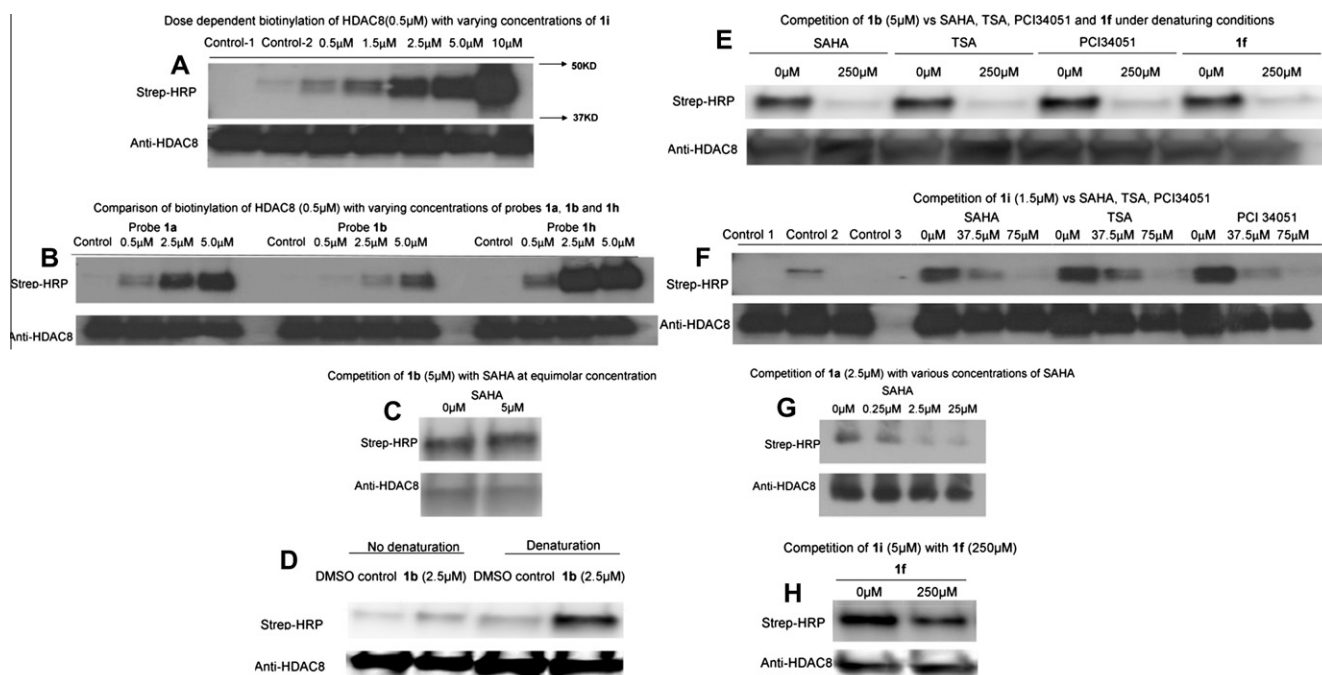


Figure 2. Characterization of biotinylated HDAC8 protein and total HDAC8 protein. (A) Western blot analysis of probe **1i** binding to HDAC8 using Strep–HRP and anti-HDAC8 antibodies, control 1–HDAC8 (0.5 μM), click reagents, control 2–HDAC8 (0.5 μM), biotin tag (50 μM), click reagents, all other lanes contain different concentrations (indicated) of **1i**, biotin tag (50 μM), click reagents. (B) Western blot analysis of probes **1a**, **1b**, and **1h** binding to HDAC8 using Strep–HRP and anti-HDAC8 antibodies, control–HDAC8 (0.5 μM), biotin tag (50 μM), click reagents, all other lanes contain different probes at concentrations indicated, biotin tag (50 μM), click reagents. (C) Western blot analysis of probe **1b** binding to HDAC8 in the presence and the absence of equimolar concentration of SAHA. (D) Western blot analysis of probe **1b** binding to HDAC8 under denaturing conditions and non-denaturing conditions. (E) Western blot analysis of probe **1b** binding to HDAC8 in the presence and the absence of an excess of HDAC8 inhibitors SAHA, TSA, PCI34051, and ligand **1f**. (F) Western blot analysis of probe **1i** binding to HDAC8 in the presence and the absence of an excess of HDAC8 inhibitors SAHA, TSA, and PCI34051, control 1–HDAC8 (0.5 μM), click reagents, control 2–HDAC8 (0.5 μM), biotin tag (50 μM), click reagents, control 3–HDAC8 (0.5 μM), probe (**1i** 1.5 μM), biotin tag (50 μM), click reagents. (G) Western blot analysis of binding of probe **1a** in the presence of varying concentrations of SAHA. (H) Western blot analysis of binding of probe **1i** in the presence and the absence of excess of ligand **1f**. Click reagents in all experiments are TCEP (500 μM), TBTA (100 μM), and CuSO₄ (1000 μM). Shown are representative blots of two or more independent experiments.

used in the photolabeling experiments with click reagents. The click reagents in all the experiments are TCEP (500 μM), TBTA (100 μM), and CuSO₄ (1000 μM).¹⁹

Our photolabeling studies required probes able to differentiate between the ‘normal’ and the hypothesized ‘upside-down’ poses leading us to design and synthesis of two additional probes **1h** and **1i**. We envisioned that after crosslinking both the probes **1h** and **1i** would still be detectable by the Strep–HRP antibody if they bind ‘upside-down’ and their alkyl azide groups point toward the solvent and can react with the alkyne-containing biotin tag via (3+2) cycloaddition. If **1h** and **1i** bind with their ester group near the zinc atom of HDAC8 then the alkyl–azido ester group would be hidden in the binding site, and these ligands are not expected to react with the alkyne moiety of the biotin tag and the resulting adducts should not be recognized by the Strep–HRP antibody. In agreement with the already established SAR, the effect of different ester groups on potency was marginal, and **1h** and **1i** inhibited HDAC8 with IC₅₀ of 67.4 and 28.9 μM, respectively. We found that similar to probe **1a**,¹⁹ probes **1h** (not shown) and **1i** produce a dose-dependent increase in biotinylation of HDAC8 (Fig. 2A).

Next, we compared the dose-dependent increase in biotinylation for ligands **1a**, **1b**, and **1h** (Fig. 2B). It was expected that ligands **1a** and **1h** would produce a pronounced dose-dependent biotinylation increase, whereas **1b** would not. Consistently with the binding mode proposed, probe **1b** gave only a very low non-specific biotinylation, whereas **1a** and **1h** gave the pronounced dose-dependent biotinylation of HDAC8. To rule out the possibility of probe **1b** binding to the main catalytic site, a competition experiment was carried out at an equimolar concentration of 85-fold more potent SAHA. The presence of an equimolar concentration

of SAHA did not result in a decrease in the biotinylation signal produced by **1b** (Fig. 2C), suggesting **1b** does not bind to the main catalytic site and produces only non-specific biotinylation under non-denaturing conditions. A comparison of the density of the biotinylated bands corresponding to the HDAC8 adducts with **1a** and **1h** provided further evidence for a novel binding mode of our non-ZCG probes. Specifically, probe **1h**, which is at least ninefold less potent than probe **1a**, gave much higher biotinylation than **1a** at the same concentrations of both these probes (Fig. 2B). Although the efficiency of the (3+2) cycloaddition and the biotinylation response may depend on the geometry of the moiety bearing the azido group and its accessibility, this observation clearly indicates that the preferable binding mode of **1h** is such that its azido group is exposed to the solvent, is accessible for the (3+2) cycloaddition reaction, and the resulting biotin-containing adduct is available for recognition by the Strep–HRP.

We envisioned that denaturing the protein prior to initiating the (3+2) cycloaddition reaction in case of probe **1b** may expose the alkyl azide, which was previously buried inside the secondary binding site, thus making it more accessible to the (3+2) cycloaddition reaction. Photolabeling of HDAC8 with probe **1b** followed by reaction with the biotin tag resulted in a much higher biotinylation under denaturing conditions as compared to non-denaturing conditions as shown in Figure 2D. To further confirm that the biotinylation produced **1b** under denaturing conditions is primarily due to interaction of the probe with the binding site of HDAC8, we performed a series of competition experiments between probe **1b** and potent inhibitors SAHA, TSA, PCI34051, and ligand **1f** (Fig. 2E). All of the competitors exhibited a pronounced decrease in biotinylation of HDAC8 by **1b**. Interestingly, despite 100–1000

fold difference in potency (Table 1), the competing ligands completely decreased the biotinylation of HDAC8 only at very high concentrations (low concentrations are not shown), suggesting that the binding of SAHA, TSA, and PCI34051 to the main catalytic site only partially obstructs the binding of probe **1b** to the secondary binding site. We observed that at 50 fold molar excess **1f** also decreased the biotinylation of HDAC8 produced by **1b** in a manner comparable to competition with SAHA, TSA, and PCI34051. Considering the remarkable difference in potency between **1f** and the latter HDAC inhibitors, the outcome of this photolabeling experiment appears to strongly indicate that the binding mode of **1b** and **1f** differs from that of the ligands that have ZCG.

Next, we investigated if probe **1i** can be competed by SAHA, TSA, PCI34051, and **1f** under non denaturing conditions. We observed that similar to probe **1b**, probe **1i** could be competed out by SAHA, TSA, or PCI34051 at 25 to 50-fold molar excess concentrations as indicated in Figure 2F. The decrease in biotinylation of HDAC8 observed with **1a** and SAHA at 0.25 and 2.5 μM (Fig. 2G) is strikingly more pronounced than that observed for **1i**: SAHA/TSA/PCI34051 for both 37.5 μM and 75 μM of these ligands. These observations suggest that unlike the hydroxamate containing probe **1a**, which probably binds primarily to the main catalytic site, probe **1i** is likely to bind to a secondary binding site where its binding is only partially obstructed by the ligands binding to the main catalytic site such as SAHA, TSA, or PCI34051. This is consistent with the experiments conducted with **1b** under denaturing conditions. We also observed that ligand **1f** is able to compete out probe **1i** (Fig. 2H). Due to relatively low potency of **1f** and low solubility the competition is less pronounced than in the case of SAHA, TSA, and PCI34051. These results further support our hypothesis that the binding of **1i** and other non-hydroxamate inhibitors in Table 1 occurs to the secondary binding site as shown in Figure 1. With **1i** and other probes in this series, we could only conduct the photolabeling studies since the kinetic experiments would require concentrations of the inhibitors at which they were not soluble.

To obtain a preliminary selectivity profile for other HDAC class I isoform, we measured the inhibition of recombinant HDAC1, 2, and 3 by probes **1h** and **1i**.^{19,29} We also assessed the inhibitory effect of probe **1i** on cytoplasmic HDAC6, a representative class II HDAC isoform, vs nuclear class I HDACs by monitoring the acetylation status of α -tubulin and histone H4 in SH-SY5Y cells, respectively.³⁶ Neither **1h** nor **1i** inhibited HDAC3 at concentrations up to 66 μM , whereas HDAC1 and HDAC2 were inhibited by these ligands with IC_{50} of 111 and 72 μM and 86 and 79 μM , respectively. The binding modes of these ligands in HDAC1 and 2 are currently being investigated. Probe **1i** showed a dose dependent increase in acetylation

status of histone H4 after a 24 h treatment (Fig. 3A). Unlike the HDAC6 selective compound **18**,³⁷ probe **1i** did not inhibit the deacetylation of α -tubulin, suggesting that **1i** targets only nuclear class I HDACs.

In summary, we demonstrated that HDAC8 enzymatic activity can be inhibited by compounds that lack an active site Zn^{2+} bidentate chelating group. Although the structure and activity require further optimization, multiple lines of evidence presented in the Letter indicate that the ligands **1b**, **1c**, **1f–1i**, **2b**, and **3b** have binding modes different from those of the parent compounds **1a**, **2a**, and **3a** and are likely to be positioned ‘upside-down’ in the secondary binding site proximal to the main catalytic site. One of the most potent ‘upside-down’ inhibitors **1i** was shown to increase acetylation of H4 but not α tubulin in SH-SY5Y cells. Studies to expand the SAR presented in the Letter, to elucidate the key pharmacophore and auxophore portions, to improve the HDAC8 inhibition and selectivity, and to co-crystallize HDAC8 with the ‘upside-down’ ligands are now in progress.

Acknowledgments

This study was funded by the National Cancer Institute/NIH grant R01 CA131970 and ADDF grant #20101103. Molecular modeling was performed using the UCSF Chimera package from the Resource for Biocomputing, Visualization, and Informatics at the University of California, San Francisco (supported by NIH P41 RR-01081) and OpenEye Scientific Software, Santa Fe, NM. We thank Dr. Carol Fierke, University of Michigan, MI, for generously providing us with the plasmid for in-house expression and purification of HDAC8. We also thank Mr. Furong Sun of the University of Illinois at Urbana-Champaign for high-resolution mass spectrometry data. The Q-ToF Ultima mass spectrometer used for HRMS data was purchased in part with a grant from the National Science Foundation, Division of Biological Infrastructure (DBI-0100085).

Reference and notes

- Khan, O.; La Thangue, N. B. *Immunol. Cell Biol.* **2012**, *90*, 85.
- Mai, A.; Rotili, D.; Valente, S.; Kazantsev, A. G. *Curr. Pharm. Des.* **2009**, *15*, 3940.
- Whittaker, M.; Floyd, C. D.; Brown, P.; Gearing, A. J. *Chem. Rev.* **2001**, *101*, 2205.
- Weisburger, J. H.; Weisburger, E. K. *Pharmacol. Rev.* **1973**, *25*, 1.
- Mulder, G. J.; Meerman, J. H. *Environ. Health Perspect.* **1983**, *49*, 27.
- Groutas, W. C.; Giri, P. K.; Crowley, J. P.; Castrisos, J. C.; Brubaker, M. J. *Biochem. Biophys. Res. Commun.* **1986**, *141*, 741.
- Gilissen, R. A.; Bamforth, K. J.; Stavenuiter, J. F.; Coughtrie, M. W.; Meerman, J. H. *Carcinogenesis* **1994**, *15*, 39.
- Meerman, J. H.; Ringer, D. P.; Coughtrie, M. W.; Bamforth, K. J.; Gilissen, R. A. *Chem. Biol. Interact.* **1994**, *92*, 321.
- Suzuki, T.; Miyata, N. *Mini. Rev. Med. Chem.* **2006**, *6*, 515.
- Suzuki, T.; Miyata, N. *Curr. Med. Chem.* **2005**, *12*, 2867.
- Suzuki, T.; Matsuura, A.; Kouketsu, A.; Hisakawa, S.; Nakagawa, H.; Miyata, N. *Bioorg. Med. Chem.* **2005**, *13*, 4332.
- Curtin, M. L. *Curr. Opin. Drug Discov. Devel.* **2004**, *7*, 848.
- Khan, N.; Jeffers, M.; Kumar, S.; Hackett, C.; Boldog, F.; Khramtsov, N.; Qian, X.; Mills, E.; Berghs, S. C.; Carey, N.; Finn, P. W.; Collins, L. S.; Tumber, A.; Ritchie, J. W.; Jensen, P. B.; Lichenstein, H. S.; Sehested, M. *Biochem. J.* **2008**, *409*, 581.
- Munday, R. *Free Radic. Biol. Med.* **1989**, *7*, 659.
- Frey, R. R.; Wada, C. K.; Garland, R. B.; Curtin, M. L.; Michaelides, M. R.; Li, J.; Pease, L. J.; Glaser, K. B.; Marcotte, P. A.; Bouska, J. J.; Murphy, S. S.; Davidsen, S. K. *Bioorg. Med. Chem. Lett.* **2002**, *12*, 3443.
- Guan, J. S.; Haggarty, S. J.; Giacometti, E.; Dannenberg, J. H.; Joseph, N.; Gao, J.; Nieland, T. J.; Zhou, Y.; Wang, X.; Mazitschek, R.; Bradner, J. E.; DePinho, R. A.; Jaenisch, R.; Tsai, L. H. *Nature* **2009**, *459*, 55.
- McQuown, S. C.; Barrett, R. M.; Matheos, D. P.; Post, R. J.; Rogge, G. A.; Alenghat, T.; Mulligan, S. E.; Jones, S.; Rusche, J. R.; Lazar, M. A.; Wood, M. A. *J. Neurosci.* **2011**, *31*, 764.
- Vickers, Chris J.; Olsen, C. A.; Lemman, Luke J.; Reza Ghadiri, M. *ACS Med. Chem. Lett.* **2012**, *3*, 505.
- He, B.; Velaparthi, S.; Pieffet, G.; Pennington, C.; Mahesh, A.; Holzle, D. L.; Brunsteiner, M.; van Breemen, R.; Blond, S. Y.; Petukhov, P. A. *J. Med. Chem.* **2009**, *52*, 7003.
- Condorelli, F.; Gnemmi, I.; Vallario, A.; Genazzani, A. A.; Canonico, P. L. *Br. J. Pharmacol.* **2008**, *153*, 657.
- Muhlethaler-Mottet, A.; Meier, R.; Flahaut, M.; Bourlout, K. B.; Nardou, K.; Joseph, J. M.; Gross, N. *Mol. Cancer.* **2008**, *7*, 55.

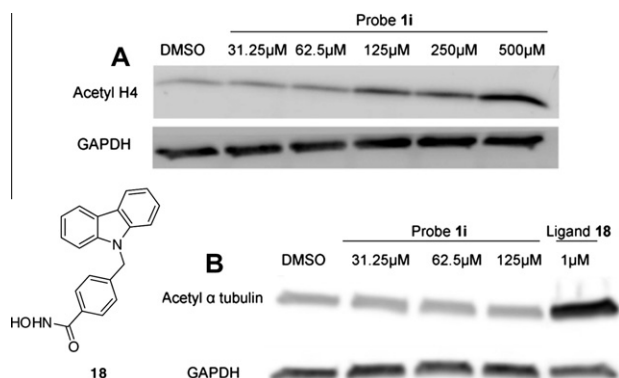


Figure 3. (A) Western blot detection of acetylation of histone H4 following a 24 h treatment with probe **1i** in SH-SY5Y cells. (B) Western blot detection of acetylation of α tubulin following a 24 h treatment with probe **1i** and ligand **18** in SH-SY5Y cells. Shown is a representative blot of two or more independent experiments.

22. Witt, O.; Deubzer, H. E.; Lodrini, M.; Milde, T.; Oehme, I. *Curr. Pharm. Des.* **2009**, *15*, 436.
23. Oehme, I.; Deubzer, H. E.; Lodrini, M.; Milde, T.; Witt, O. *Expert Opin. Investig. Drugs* **2009**, *18*, 1605.
24. Oehme, I.; Deubzer, H. E.; Wegener, D.; Pickert, D.; Linke, J. P.; Hero, B.; Kopp-Schneider, A.; Westermann, F.; Ulrich, S. M.; von Deimling, A.; Fischer, M.; Witt, O. *Lin. Cancer Res.* **2009**, *15*, 91.
25. Balasubramanian, S.; Ramos, J.; Luo, W.; Sirisawad, M.; Verner, E.; Buggy, J. J. *Leukemia* **2008**, *22*, 1026.
26. Fass, D. M.; Reis, S. A.; Ghosh, B.; Hennig, K. M.; Joseph, N. F.; Zhao, W. N.; Nieland, T. J.; Guan, J. S.; Groves Kuhnle, C. E.; Tang, W.; Barker, D. D.; Mazitschek, R.; Schreiber, S. L.; Tsai, L. H.; Haggarty, S. J. *Neuropharmacology* **2012**.
27. Somoza, J. R.; Skene, R. J.; Katz, B. A.; Mol, C.; Ho, J. D.; Jennings, A. J.; Luong, C.; Arvai, A.; Buggy, J. J.; Chi, E.; Tang, J.; Sang, B. C.; Verner, E.; Wynands, R.; Leahy, E. M.; Dougan, D. R.; Snell, G.; Navre, M.; Knuth, M. W.; Swanson, R. V.; McRee, D. E.; Tari, L. W. *Structure* **2004**, *12*, 1325.
28. **Octanoic acid (4-benzyloxyphenyl)amide (7)**. To an ice cooled solution of **6** (0.61 g, 4.2 mmol) in anhydrous dichloromethane was added EDCI (0.9 g, 4.7 mmol) followed by HOBt (0.63 g, 4.7 mmol) and stirred for 1 h. To this, was then added a solution of **4** (0.023 g, 0.14 mmol) and DIPEA (1.5 mL, 8.5 mmol) in anhydrous dichloromethane at 0 °C and stirred for 8 h. The reaction mixture was treated with 2 N aqueous HCl solution and extracted with EtOAc. The organic layer was washed with saturated aqueous NaHCO₃ solution followed by brine. The organic extracts were dried over Na₂SO₄, filtered, and concentrated under reduced pressure. The crude product was further purified by flash chromatography (90:30 → 50:50, hexanes:EtOAc) to afford **7** as a light brown solid (0.97 g, 70%). ¹H NMR (400 MHz, CDCl₃): δ 7.44–7.32 (m, 7H), 6.93 (d, J = 8.8 Hz, 2H), 5.05 (s, 2H), 2.34 (t, J = 7.6 Hz, 2H), 1.76–1.69 (m, 2H), 1.34–1.31 (m, 8H), 0.91 (t, J = 6.6 Hz, 3H). ¹³C NMR (100 MHz, CDCl₃): δ 171.4, 155.5, 136.9, 131.4, 128.6 (2C), 127.9, 127.4 (2C), 121.7, 115.1, 70.3, 37.6, 31.7, 29.3, 29.0, 25.7, 22.6, 14.1. HRMS (ESI) m/z [M+H]⁺ calcd for C₂₁H₂₈NO₂ 326.2120, found 326.2119.
- Octanoic acid [4-(3,5-dimethylbenzyloxy)phenyl]amide (1d)**. A suspension of **7** (0.95 g, 2.92 mmol) and Pd/C (150 mg, 0.14 mmol) in MeOH was allowed to react under H₂ atmosphere (balloon pressure) at rt for 5 h. The catalyst was removed by filtration through a pad of celite. The filtrate was evaporated and the white crystalline phenol **9** (0.63 g, 92%) obtained almost in pure form was directly used for next reaction.
- A mixture of **9** (100 mg, 0.42 mmol), **11** (110 mg, 0.55 mmol), and powdered K₂CO₃ (90 mg, 0.64 mmol) in acetone (10 mL) was refluxed for 6 h. The mixture was cooled to rt and concentrated leaving a residue which was dissolved in ethyl acetate and washed with water followed by brine. The organic fractions were dried over Na₂SO₄, filtered, and concentrated under reduced pressure. The crude product was purified by flash chromatography (95:05 → 80:20, hexanes:EtOAc) to furnish **1d** as a white solid (110 mg, 73%). ¹H NMR (400 MHz, CDCl₃): δ 7.49–7.41 (m, 2H), 7.06 (s, 1H), 6.98–6.92 (m, 4H), 4.97 (s, 2H), 2.35 (s, 6H), 2.34–2.31 (m, 2H), 1.75–1.69 (m, 2H), 1.37–1.31 (m, 8H), 0.91 (t, J = 7.0 Hz, 3H). ¹³C NMR (75 MHz, CDCl₃): δ 171.8, 156.0, 138.6 (2C), 137.2, 131.7, 130.0, 125.8 (2C), 122.2 (2C), 115.5 (2C), 70.8, 38.0, 32.1, 29.7, 29.5, 26.2, 23.0, 21.7 (2C), 14.5. HRMS (ESI) m/z [M + H]⁺ calcd for C₂₃H₃₂NO₂ 354.2433, found 354.2426.
- 7-[4-(3,5-Dimethyl-benzyloxy)phenylcarbamoyl]heptanoic acid methyl ester (1f)**. A mixture of **8** (100 mg, 0.36 mmol), **11** (107 mg, 0.54 mmol), and powdered K₂CO₃ (100 mg, 0.72 mmol) in acetone (10 mL) was refluxed for 6 h. The mixture was cooled to rt and concentrated leaving a residue which was dissolved in ethyl acetate and washed with water followed by brine. The organic fractions were dried over Na₂SO₄, filtered, and concentrated under reduced pressure. The crude product was purified by flash chromatography (90:10 → 80:20, hexanes:EtOAc) to furnish **1f** as a white solid (107 mg, 75%). ¹H NMR (300 MHz, CDCl₃): δ 7.42–6.92 (m, 7H), 4.97 (s, 2H), 3.67 (s, 3H), 3.33 (s, 6H), 3.32 (m, 4H), 1.73–1.62 (m, 4H), 1.40 (m, 4H). ¹³C NMR (75 MHz, CDCl₃): δ 174.2, 171.2, 155.5, 138.1 (2C), 136.7, 131.3, 129.5, 125.3 (2C), 121.6 (2C), 115.0 (2C), 70.3, 51.4, 37.2, 33.9, 28.7, 28.6, 25.4, 24.6, 21.2 (2C). HRMS (ESI) m/z [M+H]⁺ calcd for C₂₄H₃₂NO₄ 398.2331, found 398.2337.
- 7-[4-(3,5-Dimethylbenzyloxy)phenylcarbamoyl]heptanoic acid tert-butyl ester (1g)**. An ice cooled solution of **1f** (50 mg, 0.126 mmol) in THF–MeOH (5 mL, 1:1) was treated with 2 N NaOH solution (130 μL, 0.25 mmol) and the reaction mixture was allowed to stir at rt for 1 h. The reaction was diluted with ethyl acetate (10 mL) and acidified with 2 N HCl (5 mL). The organic layer was separated, dried over Na₂SO₄, filtered, and evaporated under reduced pressure. The crude acid obtained as white solid (40 mg, 85%) was directly used for next reaction without further purification.
- To a solution of acid (40 mg, 0.1 mmol) in CH₂Cl₂ (5 mL) were added oxalyl chloride (50 μL, 0.53 mmol) and one drop of dry DMF. The reaction mixture was stirred at rt for 8 h and a solution of tert-butanol (135 μL, 1.25 mmol) in CH₂Cl₂ (2 mL) and triethylamine (45 μL, 0.31 mmol) were added. The reaction mixture was stirred at rt for 12 h and concentrated under reduced pressure. The residue was purified by flash chromatography (90:10 → 70:30, hexanes:EtOAc) to give **1g** as a semi solid (20 mg, 44%). ¹H NMR (400 MHz, CDCl₃): δ 7.43–7.41 (d, J = 8.8 Hz, 2H), 7.30–7.28 (m, 1H), 7.05 (s, 1H), 6.97–6.93 (m, 4H), 4.97 (s, 2H), 2.36 (s, 6H), 2.35–2.20 (m, 4H), 1.67–1.61 (m, 4H), 1.45 (s, 9H), 1.43–1.27 (m, 4H). ¹³C NMR (100 MHz, CDCl₃): δ 173.3, 171.2, 155.6, 138.1 (2C), 136.7, 121.2, 129.6, 129.6, 125.3 (2C), 121.6 (2C), 115.1 (2C), 80.0, 70.4, 37.4, 35.4, 33.8, 28.7, 28.1 (3C), 25.4, 24.8, 21.2 (2C). HRMS (ESI) m/z [M+H]⁺ calcd for C₂₇H₃₈NO₄ 440.2801, found 440.2802.
- 7-[4-(3-Azido-5-azidomethylbenzyloxy)phenylcarbamoyl]heptanoic acid tert-butyl ester (1c)**. Compound **1c** (18 mg, 64% overall) was prepared from **1b** (50 mg, 0.107 mmol) following the same procedure described for **1g**. ¹H NMR (400 MHz, CDCl₃): δ 7.45–7.41 (d, J = 8.4 Hz, 2H), 7.16–7.09 (m, 3H), 6.94–6.92 (m, 2H), 5.05 (s, 2H), 4.38 (s, 2H), 2.36–2.34 (s, 2H), 2.23 (m, 2H), 1.75 (m, 2H), 1.61 (m, 2H), 1.46 (s, 9H), 1.40 (m, 4H). ¹³C NMR (100 MHz, CDCl₃): δ 173.2, 171.1, 155.0, 141.1, 139.8, 137.8, 131.6, 123.1, 121.6 (2C), 118.0, 117.5, 115.2 (2C), 80.0, 69.4, 54.2, 37.4, 35.4, 28.7, 28.6, 28.1 (3C), 24.9, 24.8. HRMS (ESI) m/z [M+H]⁺ calcd for C₂₆H₃₄N₇O₄ 508.2672, found 508.2673.
- (3-Amino-5-methoxyphenyl)methanol (13)**. To a solution of **12** (5 g, 0.03 mol) in anhydrous THF (100 mL) was added LiAlH₄ (2.3 g, 0.06 mol) in portions at 0 °C. The reaction mixture was stirred overnight, cooled to 0 °C, and quenched by slow addition of aqueous KOH solution (20%, 5 mL) followed by ethyl acetate (50 mL). The mixture was filtered through a pad of Celite and rinsed with ethyl acetate. The filtrate was dried over Na₂SO₄, filtered, and concentrated under reduced pressure. The crude was purified by flash chromatography (60:40 → 40:60, hexanes:EtOAc) to give compound **13** as a pale yellow solid (2.75 g, 60%). ¹H NMR (400 MHz, CDCl₃): δ 6.38 (s, 1H), 6.34 (s, 1H), 6.31 (s, 1H), 4.39 (s, 2H), 3.79 (s, 3H), 3.77 (s, 3H). ¹³C NMR (100 MHz, CDCl₃): δ 160.61, 147.49, 143.13, 105.90, 102.04, 99.87, 64.98, 54.78.
- (3-Azido-5-methoxyphenyl)methanol (14)**. To a solution of **13** (1.75 g, 11.46 mmol) in glacial acetic acid AcOH/H₂SO₄ (98% w/v)/water (4:1:5) (15 mL) was added NaNO₂ (1.58 g, 22.93 mmol) in portions at 0 °C and stirred for 10 min. NaN₃ (2.24 g, 34.4 mmol) was then added portion wise at 0 °C and the resulting mixture was stirred for 5 h at rt. The reaction was quenched with saturated aqueous NaHCO₃ solution and extracted with EtOAc (3 × 30 mL). The combined organic extracts were washed with brine, dried (Na₂SO₄), filtered, and concentrated under reduced pressure. The crude was purified by flash chromatography (70:30 → 50:50, hexanes:EtOAc) to give compound **14** as a pale yellow oil (1.88 g, 90%). ¹H NMR (400 MHz, CDCl₃): δ 6.69 (s, 1H), 6.65 (s, 1H), 6.47 (s, 1H), 4.64 (s, 2H), 3.81 (s, 3H), 2.26 (bs, 1H). ¹³C NMR (100 MHz, CDCl₃): δ 160.93, 144.02, 141.43, 109.46, 108.85, 104.02, 64.68, 55.45.
- Toluene-4-sulfonic acid 3-azido-5-methoxybenzyl ester (15)**. To a solution of **14** (1.88 g, 10.49 mmol) in anhydrous dichloromethane was added triethylamine (2.92 mL, 20.98 mmol) followed by tosyl chloride (2.20 g, 11.54 mmol) at 0 °C portion wise. The reaction mixture was stirred for 30 min at the same temperature. After completion of the reaction, the mixture was concentrated under reduced pressure and the residue was immediately purified by flash chromatography (90:10 → 80:20, hexanes:EtOAc) to give **15** as a white solid (1.75 g, 70%). ¹H NMR (400 MHz, CDCl₃): δ 7.82 (d, J = 8.2 Hz, 2H), 7.36 (d, J = 8.2 Hz, 2H), 6.58 (s, 1H), 6.50 (s, 1H), 6.47 (s, 1H), 5.01 (s, 2H), 3.78 (s, 3H), 2.47 (s, 3H). ¹³C NMR (100 MHz, CDCl₃): δ 160.91, 145.04, 141.68, 136.24, 133.09, 129.90, 127.99, 110.95, 110.39, 105.40, 71.05, 55.52, 21.66.
- 7-[4-(3-Azido-5-methoxybenzyloxy)phenylcarbamoyl]heptanoic acid methyl ester (16)**. To a solution of **15** (0.72 g, 2.15 mmol) and **8** (0.50 g, 1.79 mmol) in dry acetone (8 mL) was added K₂CO₃ (1.48 g, 10.74 mmol) at ambient temperature, and the reaction mixture was refluxed for 12 h. The mixture was poured into water and extracted with EtOAc (3 × 30 mL). The organic layer was washed with water, dried over Na₂SO₄, and evaporated under reduced pressure. The residue was purified by flash chromatography (90:10 → 70:30, hexanes:EtOAc) to afford **16** as a white solid (0.56 g, 75%). ¹H NMR (400 MHz, CDCl₃): δ (ppm) 7.43 (d, J = 8.8 Hz, 2H), 7.24 (s, 1H), 6.92 (d, J = 8.8 Hz, 2H), 6.76 (s, 1H), 6.72 (s, 1H), 6.51 (s, 1H), 5.01 (s, 2H), 3.82 (s, 3H), 3.68 (s, 3H), 2.32 (m, 4H), 1.69 (m, 4H), 1.35 (m, 4H). ¹³C NMR (100 MHz, CDCl₃): δ 174.25, 171.11, 160.99, 155.15, 141.56, 140.18, 131.57, 121.65, 115.18, 110.01, 109.51, 104.32, 69.69, 55.49, 51.51, 37.42, 33.95, 28.77, 28.31, 25.39, 24.69.
- 7-[4-(3-Azido-5-methoxybenzyloxy)phenylcarbamoyl]heptanoic acid (17)**. To a solution of **16** (0.26 g, 0.59 mmol) in THF/MeOH (1:1, 5 mL) was added 4 N KOH (0.43 mL, 1.78 mmol) at rt, and stirred for 24 h. The mixture was neutralized with 2 N HCl and extracted with EtOAc. The combined organic extracts were washed with brine, dried (Na₂SO₄), filtered, and concentrated under reduced pressure. The crude **17** obtained as a yellow solid (0.24 mg, 98%) was used for next reaction without any further purification.
- 7-[4-(3-Azido-5-methoxybenzyloxy)phenylcarbamoyl]heptanoic acid-4-azidomethylbenzyl ester (1i)**. To an ice cooled solution of **17** (0.05 g, 0.18 mmol) in anhydrous dichloromethane was added EDCI (0.038 g, 0.18 mmol) followed by HOBt (0.024 g, 0.18 mmol) and stirred for 1 h. To this, was then added a solution of [4-(azidomethyl)phenyl]methanol (0.023 g, 0.14 mmol) and DIPEA (61.3 μL, 0.35 mmol) in anhydrous dichloromethane at 0 °C and stirred for 12 h. Saturated aqueous NaHCO₃ solution was added to the reaction mixture and extracted with EtOAc. The organic layer was washed with water, dried over Na₂SO₄, and evaporated under reduced pressure. The residue was purified by flash chromatography (90:10 → 70:30, hexanes:EtOAc) to afford **1i** as a white solid (0.02 g, 68%). ¹H NMR (400 MHz, CDCl₃): δ 7.43 (d, J = 8.8 Hz, 2H), 7.38 (d, J = 8.8 Hz, 2H), 7.34 (d, J = 8.0 Hz, 2H), 7.15 (s, 1H), 6.93 (d, J = 8.0 Hz, 2H), 6.77 (s, 1H), 6.72 (s, 1H), 6.51 (s, 1H), 5.14 (s, 2H), 5.01 (s, 2H), 4.36 (s, 2H), 3.83 (s, 3H), 2.38 (t, J = 7.6 Hz, 2H), 2.31 (t, J = 7.6 Hz, 2H), 1.69 (m, 4H), 1.38 (m, 4H). ¹³C NMR (100 MHz, CDCl₃): δ 173.53, 171.03, 160.99, 155.16, 141.57, 140.18, 136.25, 135.38, 131.54, 128.65, 128.40, 121.63, 115.19, 110.01, 109.51, 104.32, 69.69, 65.66, 55.49, 55.46, 37.41, 34.15, 28.69 (2C), 25.38, 24.27. HRMS (ESI) m/z [M+H]⁺ calcd for C₃₀H₃₄N₇O₅ 572.2621, found 572.2625.
- 7-[4-(3-Azido-5-methoxybenzyloxy)phenylcarbamoyl]heptanoic acid-2-azidoethyl ester (1h)**. Compound **1h** was prepared by a coupling reaction between acid **17** and 2-azido ethanol following the same procedure described for probe **1i**. White solid, 65% yield. ¹H NMR (400 MHz, CDCl₃) δ 7.43 (d, J = 8.8 Hz, 2H), 6.93

- (d, $J = 8.8$ Hz, 2H), 6.75 (s, 1H), 6.71 (s, 1H), 6.50 (s, 1H), 5.00 (s, 2H), 4.25 (t, $J = 4.8$ Hz, 2H), 3.82 (s, 3H), 3.48 (t, $J = 4.8$ Hz, 2H), 2.38 (m, 4H), 1.69 (m, 4H), 1.40 (m, 4H). ^{13}C NMR (100 MHz, CDCl_3): δ 173.40, 171.11, 160.99, 155.15, 141.55, 140.18, 131.57, 121.67, 115.17, 110.01, 109.51, 104.31, 69.69, 62.83, 55.48, 49.80, 37.39, 33.95, 28.69, 28.69, 25.38, 24.57. HRMS (ESI) m/z $[\text{M}+\text{H}]^+$ calcd for $\text{C}_{24}\text{H}_{30}\text{N}_7\text{O}_5$ 496.2308, found 496.2318.
29. Neelarapu, R.; Holzle, D. L.; Velaparthi, S.; Bai, H.; Brunsteiner, M.; Blond, S. Y.; Petukhov, P. A. *J. Med. Chem.* **2011**, *54*, 4350.
30. Zhang, C. J.; Li, L.; Chen, G. Y.; Xu, Q. H.; Yao, S. Q. *Org. Lett.* **2011**, *13*, 4160.
31. Zhao, Y. L.; Dichtel, W. R.; Trabolsi, A.; Saha, S.; Aprahamian, I.; Stoddart, J. F. *J. Am. Chem. Soc.* **2008**, *130*, 11294.
32. Verdonk, M. L.; Cole, J. C.; Hartshorn, M. J.; Murray, C. W.; Taylor, R. D. *Proteins* **2003**, *52*, 609.
33. Brunsteiner, M.; Petukhov, P. A. *J. Mol. Model.* **2012**.
34. Photoaffinity labeling protocol: The probes or probe/competitor mixture was incubated with human recombinant HDAC8 (purified from *E. coli*) for 3 h in photolabeling buffer (25 mM Tris-HCl, pH 8.0, 137 mM NaCl, 2.7 mM KCl, 1 mM MgCl_2 , 0.1% Triton-X), exposed to 254 nm UV light 3×1 min with 1 min resting. In case of denaturation experiments, post photocrosslinking, a solution of sodium dodecyl sulfate in water was added to attain final concentration of 2% w/v. Biotin tag BT was attached to HDAC8-probe adduct using the (3 + 2) cycloaddition reaction catalyzed by TBTA and Cu(I) produced in situ from CuSO_4 and TCEP. The final concentrations of BT, TCEP, TBTA, and CuSO_4 are 50 μM , 0.5 mM, 0.1 mM, and 1 mM respectively. After 60 min of incubation at rt, protein samples were analyzed by SDS-PAGE and western blot using an antibiotin primary antibody, streptavidin conjugated to horseradish peroxidase (Pierce, Rockford, IL), and ECL (Pierce, Rockford, IL). The membranes were then stripped in 0.2 M glycine, pH 2.6 for 10 min, and then in 0.2 M glycine, pH 2.3 for another 10 min, before being reblocked and redecorated with an anti-HDAC8 primary antibody and an antirabbit-HRP secondary antibody. Western blotting was done with 0.5 μg of purified protein with $5 \times$ loading buffer containing 10% SDS, 0.05% bromophenol blue, 50% glycerol, and β -mercaptoethanol. Protein samples were boiled for 5 min and allowed to cool before loading on a denaturing 10% polyacrylamide gel electrophoresis (SDS PAGE). After electrophoresis, protein was transferred to a polyvinylidene difluoride membrane (Imobilon-Millipore, Bedford, MA). The membrane was incubated for 1 h with 3% albumin fraction V (USB, OH) and washed three times with 1x phosphate buffer saline supplemented with 0.1% of Tween-20 (PBS-T). The membrane was then incubated with an anti-HDAC8 antibody (1:3000) for 1 h under rt with slight agitation. After three washes in PBS-T, the membranes were incubated with a secondary antibody antirabbit-HRP for 1 h at rt. The signals were detected using the enhanced chemiluminescence (ECL) kit from Pierce (Pierce Biotechnology, Rockford, IL).
35. Dowling, D. P.; Gattis, S. G.; Fierke, C. A.; Christianson, D. W. *Biochemistry* **2010**, *49*, 5048.
36. Cell Culture and western blot protocol: SH-SY5Y cells seeded at 1.0×10^5 cells/well in 6 well plates and grown to 80% confluence in 1:1 DMEM:OPTI-MEM (Gibco) supplemented with 10% FBS (Gibco), 1% Antibiotic-Antimycotic (Gibco), and 1% penicillin-streptomycin (Mediatech). Cells were treated with either vehicle, increasing concentrations of **1i**, or HDAC6-selective compound **18**. Cells were maintained at 37 °C and 5% CO_2 for 24 h after treatment. Cells were lysed using $1 \times$ RIPA buffer (150 mM NaCl, 1% Triton X-100, 0.5% sodium deoxycholate, 0.1% SDS, 50 mM Tris, pH 8.0) containing 1:100 dilutions of protease inhibitor cocktail (Sigma) and 1:100 dilution of phosphatase inhibitor (Sigma) with shearing. Lysates were clarified through centrifugation at 13,000 rpm at 4 °C. Total protein concentration was determined via the BCA Protein Assay Kit (Pierce). Lysates were stored at -20 °C until later use. Sample vials were prepared by aliquoting 20 μg of total protein and adding $4 \times$ Sample Buffer with 10% β -mercaptoethanol. Sample vials were boiled for 5 min, cooled to RT, and separated by gel electrophoresis at 80 V. Proteins in the gel were transferred to PVDF membrane in 4 min using the Invitrogen iBlot system. Membranes were blocked using 5% Milk in PBS-T and probed using anti-GAPDH (1:5000), anti-acetyl α -tubulin, or anti-acetyl histone H4 (1:1000) overnight at 4 °C. Membranes were incubated with either anti-mouse (1:5000) or anti-rabbit (1:5000) in 5% milk in PBS-T. Results were visualized using Femto chemiluminescent substrate (Pierce) in CCD camera. HRP-conjugated anti-rabbit IgG (H+L) was purchased from GE (Piscataway, NJ). Anti-acetyl α -tubulin was purchased from Santa Cruz Biotechnology (Santa Cruz, CA). All other antibodies (anti-GAPDH, anti-acetyl histone H4, and HRP-conjugated anti-mouse IgG (H+L)) were purchased from Millipore.
37. Butler, K. V.; Kalin, J.; Brochier, C.; Vistoli, G.; Langley, B.; Kozikowski, A. P. *J. Am. Chem. Soc.* **2010**, *132*, 10842.